

# Using Sensitivity Analysis and Optimization for Civil Engineering and Geotechnical Applications

Heinz Konietzky<sup>1</sup>, Roger Schlegel<sup>2</sup>

<sup>1</sup> TU Bergakademie Freiberg, Institut für Geotechnik, Professur für Gebirgs- und Felsmechanik/Felsbau

<sup>2</sup> DYNARDO – Dynamic Software and Engineering GmbH, Weimar

**Keywords:** sensitivity analysis, pareto-optimization, geotechnical anchor scheme, masonry arch bridge

# 1 INTRODUCTION

Der Einsatz moderner numerischer Simulationsverfahren ermöglicht heute die Untersuchung komplexer Strukturen welche unterschiedlichsten Beanspruchungen ausgesetzt sein können. Durch die Verwendung leistungsfähiger Elementformulierungen, Materialmodelle und Solver können Strukturantworten unter Einbeziehung hochgradig nichtlinearen Verhaltens bis in den Versagensbereich hinein simuliert werden. Die Konsequenzen dieser progressiven Entwicklung im Bereich der numerischen Simulationen liegen u.a. in der immer umfassenderen Einbeziehung verfügbarer Informationen in den Simulationsprozess und in der Berechnung immer komplexerer Strukturen deren Auslegung, Dimensionierung oder Ist-Zustandsbewertung oftmals die Erschließung nichtlinearer Tragreserven beinhaltet. Strukturen werden dabei immer mehr bis an die Grenzen ihrer Tragfähigkeit und Gebrauchstauglichkeit ausgelastet.

Die Beherrschbarkeit und Kontrollierbarkeit derartiger Strukturanalysen erfordern einen hohen Automatisierungsgrad. Zur Gewährleistung des gewünschten Sicherheitsniveaus der Strukturauslegung sowie zur Überprüfung der notwendigen Robustheit der numerischen Analyse wird es notwendig die Abhängigkeit der Strukturantwort einerseits von unvermeidbaren, in der Natur vorkommenden Streuungen von Inputparametern und andererseits von gezielten Variationen von numerischen Parametern und Solvereinstellungen zu untersuchen. CAE-gestützte Optimierung und CAE-gestützte Sensitivitätsanalyse sind dabei wesentliche Bestandteile.

Wie in anderen Industriezweigen erzwingt auch im Bauwesen und in der Geotechnik der inzwischen internationale Konkurrenzdruck die immer kostengünstigere Herstellung besonders zuverlässiger und ökologisch verträglicher Produkte. Die Kombination moderner numerischer Simulationsverfahren und CAE-gestützter Optimierungsmethoden ermöglicht hierbei eine effektivere virtuelle Produktentwicklung und die Erschließung vorhandener Kostenpotentiale. Der vorliegende Beitrag zeigt an Hand von ausgewählten Beispielen den Einsatz von mathematischen Optimierungsverfahren und Sensitivitätsanalysen im Bauwesen und in der Geotechnik auf.

## 2 EXAMPLE: OPTIMIZATION OF AN ANCHOR SCHEME

To demonstrate the general procedure of a combined sensitivity and optimization analysis, a simple, but typical mining application was used: the roof support of a drift by anchors.

How the intended support behaves depends on several parameters like type of anchor, distance between anchors, length of anchors, material parameters of anchor, constitutive behaviour of rock mass, depth below surface, geometry of opening, geological conditions, characteristics of grout etc. All these and other parameters have a more or less significant influence on the system behaviour. For the further steps (optimization, robustness assessment, safety analysis ...) it is

essential to know the importance of these parameters on the system behaviour. The sensitivity analysis answers this question. The most important (critical) impact parameters will be detected and less important or unimportant parameters can be excluded from further studies.

Based on this sensitivity analysis an optimization analysis follows. To perform an optimization evaluation criteria objectives for the optimization have to be defined. If one single objective with multiple criterions is defined, the single objective optimization ends with one result (optimum). However, in some cases two or more criteria exist, which are contradictory and therefore no single optimum, but a set of PARETO optimal solutions exist. The below given simple example uses the maximum roof displacement (safety criterion) and the minimum total anchor length (economic criterion) as optimization criteria.

To demonstrate the whole procedure a simple 2-dimensional numerical model as shown in Fig. 1 was used. The model represents half of a chamber 10 m wide and 5 m high. Due to the symmetry conditions a half-space model was used. The model has a vertical symmetry line at the left boundary and contains 5 roof anchors. The rock mass was modeled using the classical elasto-plastic Mohr-Coulomb model with tension cut-off and non-associated flow rule. The virgin principal stress state is characterized by 10 MPa vertical stress and 5 MPa horizontal stress. The outer model boundaries are fixed in the normal direction. Parameters are given in Tab. 1.

Parameter	Description	Unit	Value
<b>Rock mass</b>			
E	Young's-modulus	Pa	$10^9$
v	Poisson's ratio		0,3
$\varphi$	Friction angle	$^\circ$	30
$\psi$	Dilation angle	$^\circ$	10
c	Cohesion	Pa	$10^5$
f <sub>t</sub>	Uniaxial tensile strength	Pa	0
$\rho$	Density	kg/m <sup>3</sup>	2500
<b>Anchor</b>			
length_anker1-5	Anchor length 1 – 5	m	5
dxdirec	Distance between anchors	m	1
e_anker	Young's modulus of anchor steel	Pa	$10^{10}$
yield_anker	Yield point of anchor steel	Pa	$10^7$
radius_anker	Anchor radius	m	0,01
<b>Interaction between anchors and rock mass (FLAC, 2006)</b>			
cs_ncoh / scoh	Cohesion normal / shear	Pa	$10^5 / 10^5$
cs_sfrc	Friction angle	$^\circ$	10
cs_nstiff / sstiff	Grout stiffness normal / shear	Pa	$10^7 / 10^7$
grout_thick	Grout thickness	M	0,01

Tab. 1 Basic parameter set for rock mass, anchor and grout

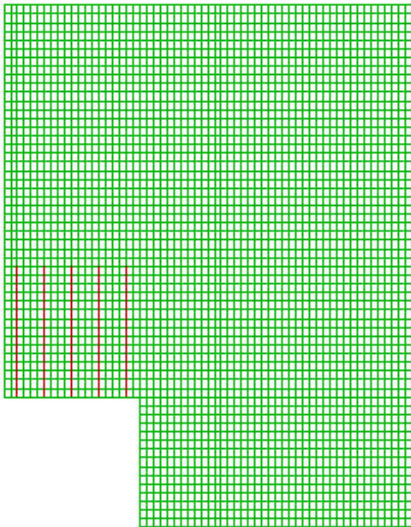


**Fig. 1 Model set up: numerical mesh with installed rockbolts**

## 2.1 Sensitivity analysis

First of all, a sensitivity analysis was performed to investigate the impact of the individual parameters on the roof subsidence. The most important parameters according to Tab. 2 were used. A stochastic sampling method, the Latin Hypercube sampling, was used to define the input parameter sets. Only 50 model runs were necessary to derive the linear and quadratic correlation coefficients and coefficients of determinations, respectively.

Exemplary, the Anthill-Plot for the anchor length versus the obtained maximum roof settlement is shown in Fig. 3.

Name	Description	Unit	Lower Bound	Upper Bound
length_anker	length of anchor	M	1,0	5,0
radius_anker	radius of anchor	M	0,01	0,1
e_anker	E-Modul of anchor	Pa	$10^{10}$	$2,0 * 10^{11}$
cs_ncoh	grout normal cohesion	Pa	$10^5$	$5,0 * 10^6$
cs_scoh	grout shear cohesion	Pa	$10^5$	$5,0 * 10^6$
cs_sflic	friction angle	°	10	60
cs_ssstiff	grout shear stiffness	Pa	$10^7$	$10^8$
cs_nsstiff	grout normal stiffness	Pa	$10^7$	$10^8$
yield_anker	yield stress of anchor material	Pa	$10^8$	$10^9$
grout_thick	grout thickness	m	0,01	0,1

**Tab. 2 Input parameters with lower and upper bounds for sensitivity analysis**

The example is based on the simplified assumption, that all anchors have the same length and that the distance between the anchors is fixed. The plot of the coefficient of determination of the maximum roof settlement (Fig. 2) shows, that 60% of the roof settlements can be explained by the anchor length alone. All other

input parameters have less than 40% influence. As expected the maximum roof subsidence decrease with increasing anchor length.

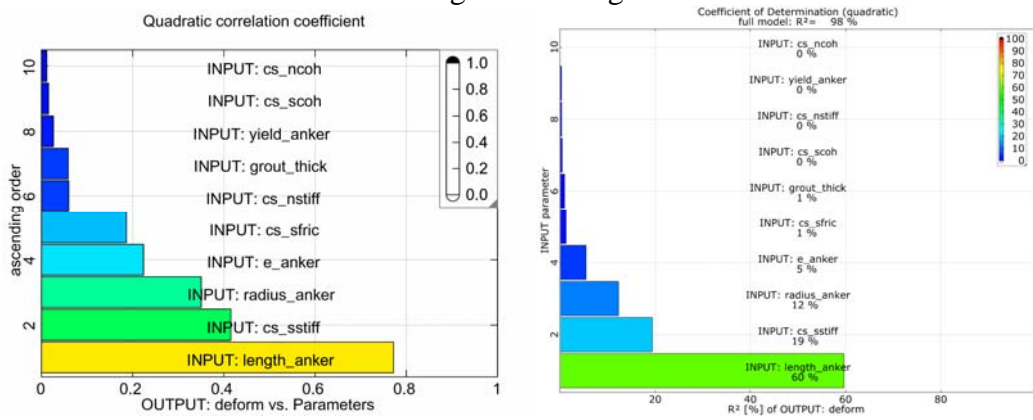


**Fig. 2 Quadratic correlation coefficients and coefficients of determination**

INPUT: length\_anker vs. OUTPUT: deform, (linear)  $r = 0.772$

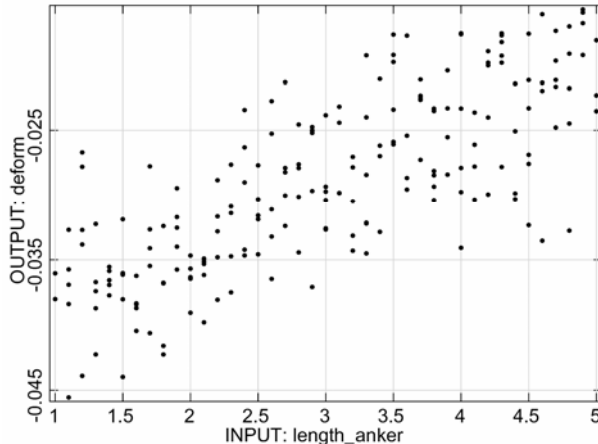


**Fig. 3 Anthill-plot: anchor length (m) versus output (maximum roof settlement; m)**

Name	Description	Unit	Lower Bound	Upper Bound
length1	length of anchor 1	m	1,0	5,0
length2	length of anchor 2	m	1,0	5,0
length3	length of anchor 3	m	1,0	5,0
length4	length of anchor 4	m	1,0	5,0
length5	length of anchor 5	m	1,0	5,0
dxdirec1	distance between symmetry axis and anchor 1	m	0,25	2,5
dxdirec2	distance between anchor 1 and 2	m	0,5	2,5
dxdirec3	distance between anchor 2 and 3	m	0,5	2,5
dxdirec4	distance between anchor 3 and 4	m	0,5	2,5
dxdirec5	distance between anchor 4 and 5	m	0,5	2,5

**Tab. 3 Input parameters with lower and upper bounds for sensitivity analysis**

Based on the knowledge, that the anchor length plays a dominate role, a second sensitivity analysis was performed, there both, the parameters for the rock mass as

well as the parameters for the interaction between the rock mass and the anchors were fixed. Instead of fixed anchor locations, now the anchors are allowed to move along the roof and the anchor length can be different for each anchor within the values of 1 to 5 m, Tab. 3.

This sensitivity analysis shows that the anchors 1 and 2 have by far the strongest influence on the roof subsidence. The length of the anchor 5 (nearest to the side wall) shows no correlation to the maximum roof subsidence, Fig. 4 and Fig. 5.

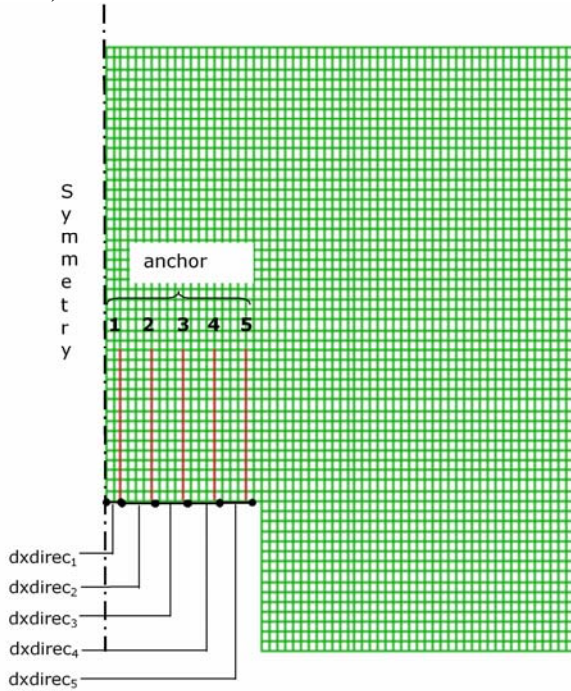


**Fig. 4 Numerical model set-up**

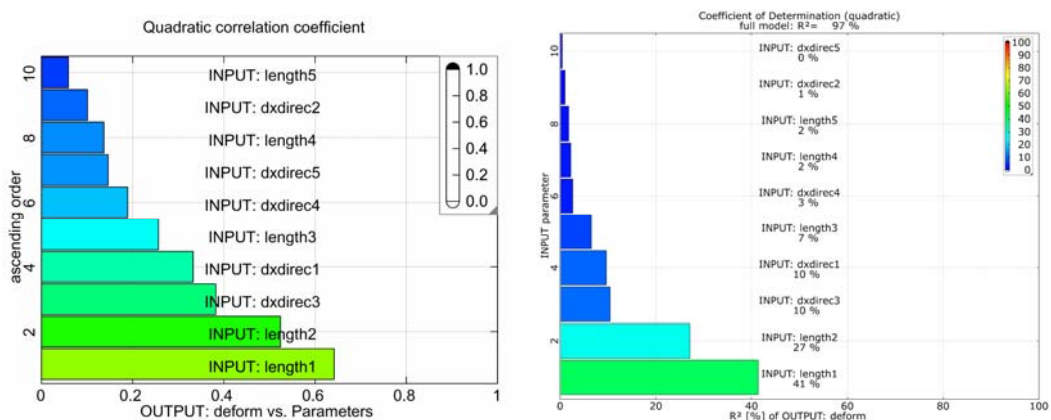


**Fig. 5 Quadratic correlation coefficients and coefficients of determination**

## 2.2 Optimization

Based on the results of the sensitivity analysis, an optimization based on evolutionary algorithms was performed. A quite interesting approach is the Pareto-Optimization, where several contradictory objective functions are defined. Besides the technical (safety) objective  $f_1$  (= maximum allowable roof settlement) a second economic objective  $f_2$  (= minimum of total anchor length) was defined:

first objective

$$f_1 = \text{maximum roof subsidence} \rightarrow \min$$

second objective:

$$f_2 = \sum_{i=1}^5 l_i \rightarrow \min$$

with the constraint:

$$\sum_{i=1}^5 dx_{direc_i} \leq 4,5m$$

1000 runs were performed. The Pareto-Optimization automatically results in the maximum anchor length (5 x 5m) at the left upper corner and minimum anchor length (5 x 1m) at the right lower corner of the Pareto-front (see Fig. 6). The best design gives an accumulated anchor length of 11 m for 2.5 cm roof subsidence (see Fig. 7).

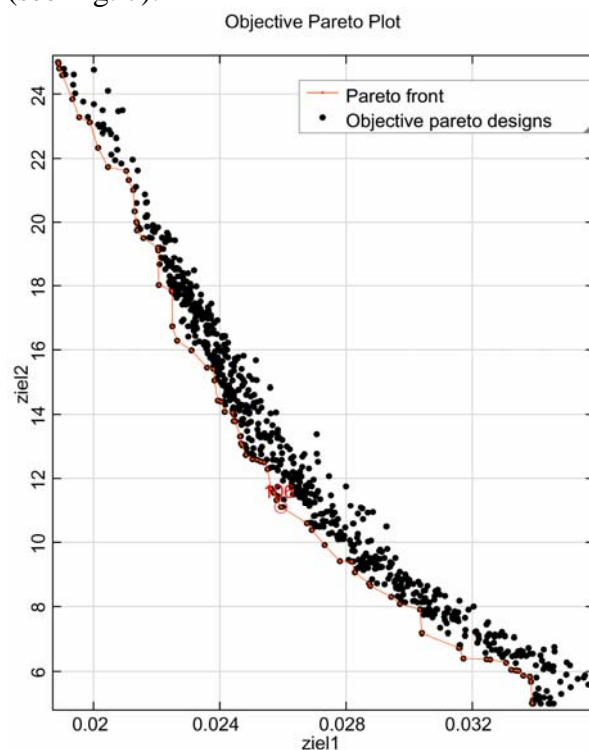


**Fig. 6 Roof settlement [m] versus accumulated anchor length [m]**

Along the Pareto-front all other optimum designs can be obtained. The minimum roof subsidence is reached with the anchor lengths  $l_{1-5} = 5$  m and the respective minima for the anchor distances.

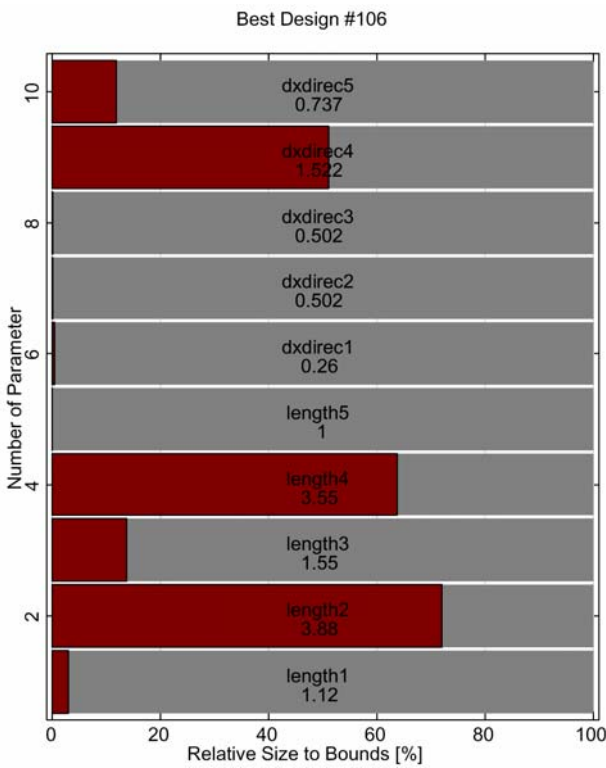


**Fig. 7 Parameters for best design**

The interesting point is, that both anchor length and location are strongly inhomogeneous for the optimum designs. This is caused by the inhomogeneous secondary stress field, the non-linearities of rock behaviour (plastifications) and the interaction between rock mass and anchors.

### 3 ANALYSIS OF A MASONRY ARCH BRIDGE

The examined railway viaduct and the different material areas are presented in Fig. 8. The length of the arch bridge is 103,62 m and the height approx. 30 m.



**Fig. 8 Masonry arch bridge (left), material areas (right)**

The load bearing capacity of the structure should be calculated for the actual state and the serviceability of masonry arches should be tested for current life loads. The arches are made of regular sandstone masonry.

The spandrel walls and the piers exist of quartzite schist masonry. The piers normally consist of multiple layers of regular and irregular masonry. No exact materials are defined for the stiffness and the strength of masonry. They should be defined by corresponding tests and material examination. The calculations described below are necessary for the localisation of relevant areas for taking the samples and for the identification of relevant material parameters. Therefore, the order of the material variables is estimated in respect of lower and upper limits with the help of the literature and different codes (DIN 1053, Eurocode 6, UIC-Kodex 778-3 E).

For the determination of significant life load positions, the train passage over the bridge was simulated by using estimated mean material variables. Fig. 9 shows the most inconvenient life load position for the arch load.

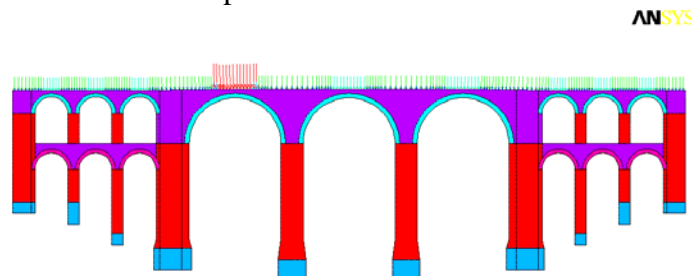


**Fig. 9 Relevant life load position**

The sensitivity analysis is carried out in the service load status and help to determine the failure load. Thus, the service load status is calculated with nonlinear load history calculations with three load steps:

- 1: dead loads
- 2: temperature pressure in winter time
- 3: life load according to Fig. 9

For the determination of the failure load, as follow-up the life load is increased until the bridge failures.

### 3.1 Sensitivity analysis

The sensitivity analysis was done for the 21 most important scattered, independent material variables of different material areas which is shown in Fig. 8 (right). These are the e-moduli of the arch masonry  $ey_1$ ,  $ey_5$ , the spandrel walls  $ex_2$  and the pier  $ex_3$ , the masonry compression strength  $fmx_1$ ,  $fmx_2$ , the tensile strength  $ftx_1$ ,  $ftx_2$ ,  $ftx_5$ , the shear strength variables, the friction angle  $\phi$  and cohesion  $c$ , the joint distances of the horizontal joints  $al_1$ ,  $al_2$ ,  $al_5$  and the vertical joints  $as_y1$ ,  $as_y2$ ,  $as_y5$  as well as the density of the material areas  $roh_1$ ,  $roh_2$ ,  $roh_3$ ,  $roh_5$ .

The aim of the sensitivity analysis is the examination of the sensitivity of the response values according Tab. 1 and failure load on the variation of material parameters. It is obligatory for a significant statistic analysis to represent the

design space equally, that means an equal representation of the upper and lower bounds of the parameters. Thus, optiSLang offers efficient methods.

In this case, the Latin Hypercube Sampling (LHS) was used as random sample plan (DOE scheme). LHS is a stratified sampling methodology which divides the parameter distribution into equal probability intervals. The parameters within the interval are chosen by chance. The LHS technique tries to represent the design space equally by minimising the variation of distance vectors. This secures an optimal random sample density over the entire parameter space for the statistic analysis. Each parameter is supposed to be uniformly distributed. 199 Designs were calculated for the sensitivity analysis.

The statistic sensitivity analysis utilizes linear and quadratic correlation matrixes, its corresponding correlation coefficients and the coefficients of determination of the response parameters. The linear (or quadratic) correlation coefficient can show the degree of an statistic linear (or quadratic) correlation between input and response parameters. It indicates how two databases correspond linearly (or quadratically) and states to what extend they depend on each other linearly (or quadratically).

### 3.1.1 Sensitivity of serviceability

For the evidence of the serviceability, stresses and deformations are especially interesting. Therefore, the arch stresses and vertical deformations of masonry and the horizontal compression strength of the spandrel wall masonry are chosen as response parameters for the sensitivity analysis (see Tab. 4). The qualitative distribution of vertical deformations are shown in Fig. 10 (left) and in Fig. 10 (right) the arch and horizontal stresses are presented.

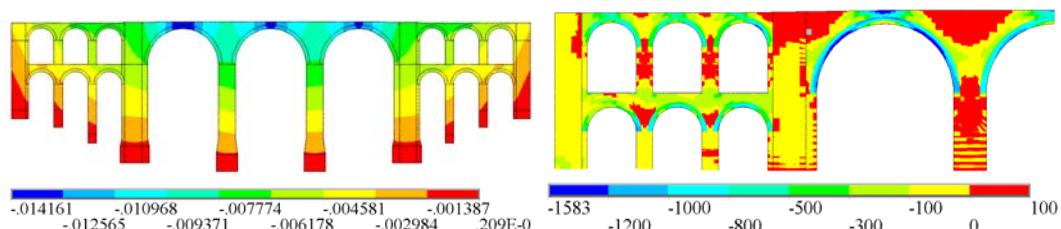


**Fig. 10 Response values under service load level** left: vertical displacements (m), right: arch and horizontal stresses (kN/m<sup>2</sup>)

Response value	description
z1	vertical total displacements of masonry arch crown, level 1
z2	vertical relative displacements of masonry arch crown, level 1
z3	maximal arch compression stress, arch level 1
z4	compression stress of masonry arch crown, level 1
z6	maximal horizontal compression stress, spandrel walls

**Tab. 4 Response parameter**

Response	mean value	minimum	maximum	CoV	CoD lin[%]	CoD quad [%]
z1	-0.0135 m	-0.0177 m	-0.0109 m	0.1	93.0	99.0
z2	-0.0080 m	-0.0094 m	-0.0070 m	0.063	86.0	94.0
z3	-1540.0 kN/m <sup>2</sup>	-2440.0 kN/m <sup>2</sup>	-1090.0 kN/m <sup>2</sup>	0.164	85.0	92.0
z4	-1220.0 kN/m <sup>2</sup>	-2440.0 kN/m <sup>2</sup>	-497.0 kN/m <sup>2</sup>	0.374	96.0	98.0
z6	-1850.0 kN/m <sup>2</sup>	-2940.0 kN/m <sup>2</sup>	-717.0 kN/m <sup>2</sup>	0.294	97.0	99.0

**Tab. 5 Results for the Response parameter (CoV – Coefficient of Variation, CoD – Coefficient of Determination)**

The results for the response values are listed in Tab. 5. The linear correlation matrix is shown in Fig. 11 (left). It is a symmetric matrix that includes linear correlation coefficients. The size of the correlation coefficients show relevant material parameters with high influence on the response parameters and can be read from the matrix. In Fig. 11 (right), the correlation coefficients of the material parameters are stated for the vertical relative displacements of masonry arch crown. In Fig. 12 (left) are shown the corresponded coefficients of determination. As expected, E-modul ey\_1 of arch masonry has the highest impact on the vertical bending. The linear correlation coefficient  $r$  is 0,73 and the coefficient of determination is  $R^2 = 54\%$ . That means 54 % of the change of the arch bending can be explained by the distribution of ey\_1. Further material parameter with relevant correlation are ex\_2 ( $R^2 = 10\%$ ) and phi ( $R^2 = 7\%$ ). In Fig. 12 (right), the linear correlation coefficients of material parameters are stated for the maximal arch compression stress. Here, the three most important material parameters are ex\_2 ( $R^2 = 49\%$ ), ey\_1 ( $R^2 = 38\%$ ) and phi ( $R^2 = 8\%$ ). As a result, the e-moduli of the arch masonry and the spandrel walls as well as the friction angle are the most important material parameters for the evidence of the serviceability. The resulting correlation between ey\_1 and z2 is presented in Fig. 13 (left) as anthill plot. Fig. 13 (right) shows the resulting correlation between ex\_2 and z3.

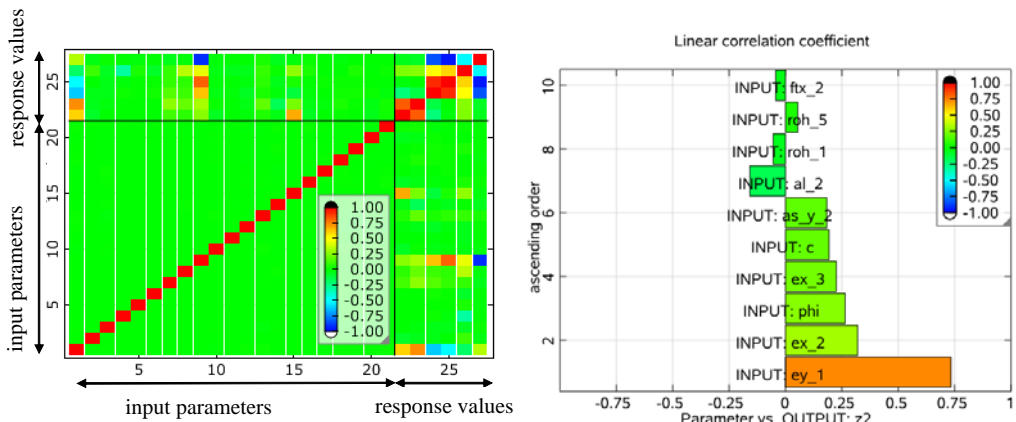


**Fig. 11 Left: linear correlation matrix, service load level; right: linear correlation coefficients, response z2– relative vertical displacement of the arch crown**

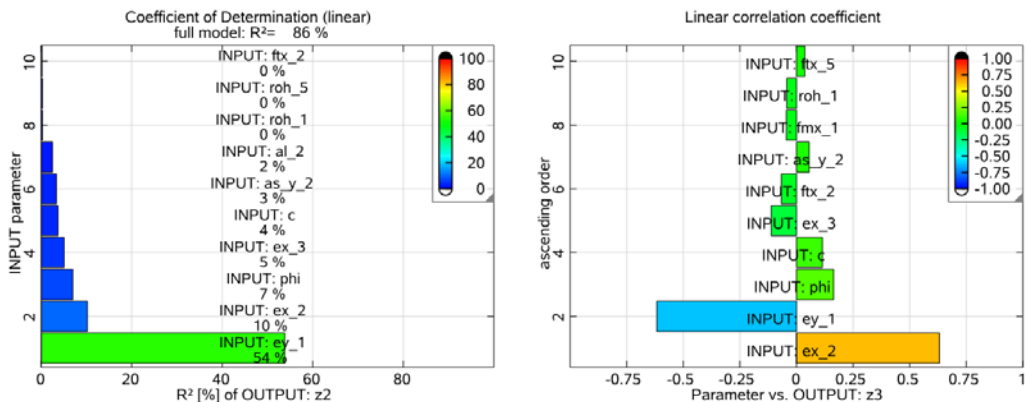


**Fig. 12 Left: coefficient of determination, response z2; right: linear correlation coefficients, response z3**

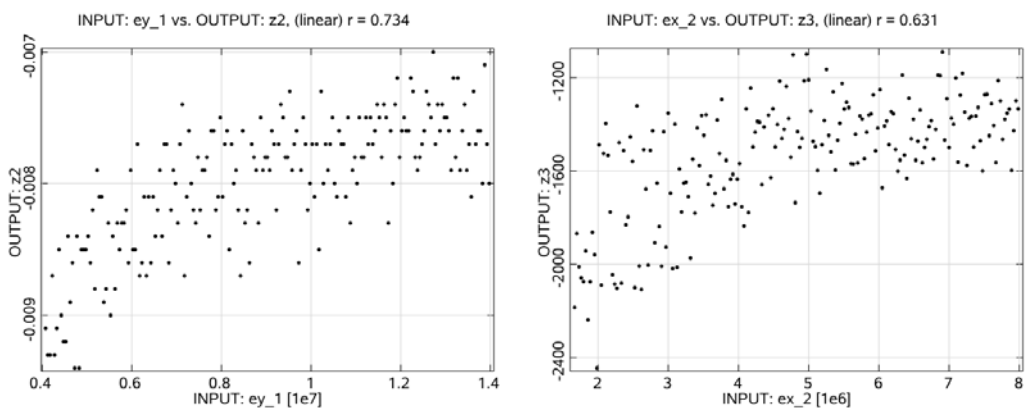


**Fig. 13 Left: anthill plot response z2 vs. input ey\_1 (kN/m<sup>2</sup>); right: anthill plot response z3 vs. input ex\_2 (kN/m<sup>2</sup>)**

### 3.1.2 Sensitivity of the failure load

The found failure mechanisms on reaching the failure load are displayed in Fig. 14. It becomes obvious that the failure of the structure is described by a lateral evasion of the arch bearing over the pier, a failure of the spandrel walls and a failure of arch masonry.

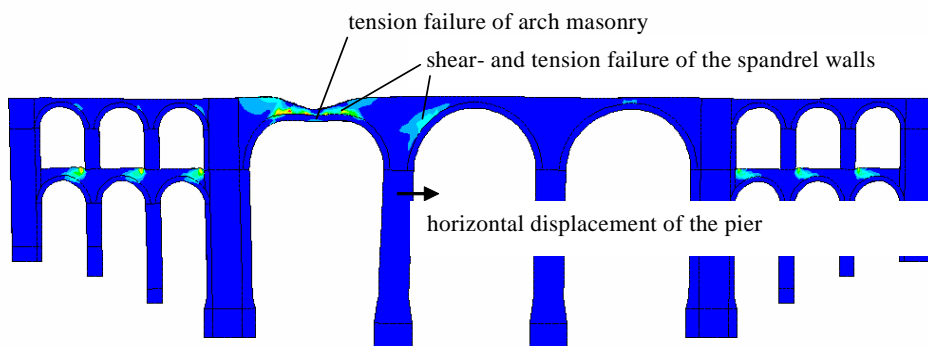


**Fig. 14 Plastic strains and failure mechanisms**

The statistic evaluation shows that only 74% of the entire distribution of the failure load can be explained by linear correlation coefficients. For quadratic correlation the coefficient of determination is 96%. Therefore, the quadratic correlation coefficients in Fig. 15 (left) have to be involved. The failure is obviously highly influenced by ex\_3 (e-modul of the pier masonry  $R^2 = 23\%$ ) and with that by the horizontal move of the pier head. Further relevant material parameters are e-modul ey\_1 ( $R^2 = 16\%$ ) and the compression strength fmx\_1 ( $R^2 = 14\%$ ) of masonry as well as ftx\_2 and phi for the failure load of arches. Fig. 15 (right) shows the resulting distribution of the response failure load in a histogram.

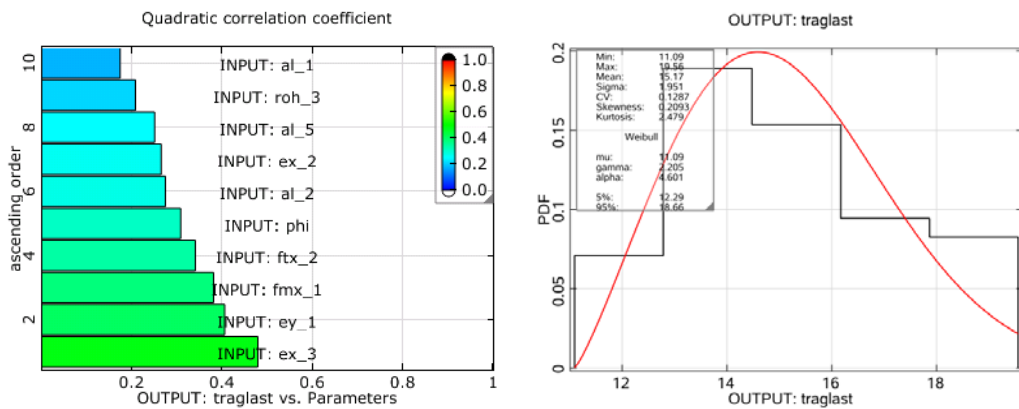


**Fig. 15 Left: quadratic correlation coefficients of the most important parameters; right: Histogram failure load**

## 4 CONCLUSIONS

Auch im Bauwesen und in der Geotechnik können CAE-gestützte Sensitivitätsanalysen und Optimierungen sehr vorteilhaft eingesetzt werden. Sensitivitätsanalysen zeigen deutlich die Abhängigkeiten und Trends zwischen Inputparametern und Strukturantworten im Simulationsmodell auf und sind damit eine notwendige Grundlage für die Formulierung eines Optimierungsproblems. Ebenso werden sie häufig zur Kontrolle komplexer Modelle und zur Schärfung des Problemverständnisses verwendet.

Das Einsatzspektrum der Optimierung im Bauwesen und der Geotechnik ist sehr umfangreich und reicht von der Produktoptimierung an sich über die Optimierung der Konstruktion bis hin zur Parameter- und Systemidentifikation.

## REFERENCES

SCHLEGEGL, R., KONIETZKY, H. & WILL, J. Optimization and Sensitivity Analysis in Mining and Geotechnical Engineering using Numerical Approaches, Buletin Resurse Minerale, Volume 2, 2007, p. 47-54

FLAC 2006. ITASCA CONSULTING GROUP, MINNEAPOLIS, MINNESOTA, USA,  
[WWW.ITASCA.DE](http://WWW.ITASCA.DE).

optiSLang (2006). The optimizing Structural Language; Dynardo GmbH ;  
[www.dynardo.de](http://www.dynardo.de).